2.3 Flow Separation and Frontal waves.

If the fluid depth goes to zero over a finite portion of the channel cross section, the interface or free surface forms a free edge or 'front'. Arguments presented in the previous section prove that this grounding must first occur at the left sidewall (Figure 2.1b), provided that the potential vorticity is non-negative. Separation of the layer from the left wall means that the corresponding Kelvin wave is replaced by a new 'frontal' wave whose properties are quite different from its predecessor. This twofold behavior is an artifact of the rectangular channel geometry; real ocean straits have continuously varying *h* and layer thickness that always vanishes at the edges. However, the inconvenience in treating attached and detached flows separately is minor compared to the technical difficulties in dealing with smooth cross-sections (e.g. Section 2.8).

For detached flow it is not necessary to re-derive the depth and velocity profile; one can simply modify the old ones. In doing so, the reader should keep in mind that (2.2.3) and (2.2.4) remain valid when the depth just vanishes at the left wall. For a flow that is separated, one can place an imaginary wall at the free left edge and adjust the coordinate to conform to the imaginary channel. Since (2.2.3) and (2.2.4) assume symmetry in the position of the channel walls about x=0, we replace x by, x-x_c where $x_c = (w - w_e(y,t))/2$ is the midpoint of the separated current. The edges of the current now lie at $x - x_c = \pm w_e/2$ and the condition of vanishing depth at the left edge implies $\hat{d} = \overline{d} = \frac{1}{2}d(w/2, y, t)$. The new depth and velocity are then given by

$$d(x,y,t) = q^{-1} + \overline{d}(y,t)\frac{\sinh[q^{1/2}(x - x_c(y,t))]}{\sinh(\frac{1}{2}q^{1/2}w_e(y,t))} + (\overline{d}(y,t) - q^{-1})\frac{\cosh[q^{1/2}(x - x_c(y,t))]}{\cosh(\frac{1}{2}q^{1/2}w_e(y,t))}. \tag{2.3.1}$$

and

$$v(x,y,t) = q^{1/2}\overline{d}(y,t)\frac{\cosh[q^{1/2}(x - x_c(y,t))]}{\sinh(\frac{1}{2}q^{1/2}w_e(y,t))} + q^{1/2}(\overline{d}(y,t) - q^{-1})\frac{\sinh[q^{1/2}(x - x_c(y,t))]}{\cosh(\frac{1}{2}q^{1/2}w_e(y,t))}. \tag{2.3.2}$$

From these expressions follow modified versions of (2.2.7) and (2.2.8):

$$\overline{v} = q^{1/2}T_e^{-1}\overline{d} \tag{2.3.3}$$

and

$$\hat{v} = q^{1/2}T_e(\overline{d} - q^{-1}), \tag{2.3.4}$$

where $T_e = \tanh(\frac{1}{2}q^{1/2}w_e(y,t))$.

One may now repeat the steps outlined in the previous section to obtain equations governing the evolution of the free edge $x = \frac{1}{2}w(y) - w_e(y,t)$. Begin by writing the y-momentum equation at the free edge and using the kinematic condition

$$\frac{\partial v(\tfrac{1}{2}w(y)-w_e(y,t),y,t)}{\partial t}=\left[\frac{\partial v}{\partial t}\right]_{x=const.}-\left[\frac{\partial v}{\partial x}\right]_{x=\frac{1}{2}w-w_e}\frac{\partial w_e}{\partial t}. \qquad (2.3.5)$$

The result is

$$\frac{\partial v_e}{\partial t}-\frac{\partial w_e}{\partial t}+\frac{\partial}{\partial y}\left(\frac{v_e{}^2}{2}+h\right)=0, \qquad (2.3.6)$$

where v_e is the value of v at the free edge.

To the momentum equation written along the right wall (2.2.13 with the '+' sign) one now subtracts or adds (2.3.6), resulting in

$$\frac{\partial[q^{1/2}T_e(\bar{d}-q^{-1})]}{\partial t}+\tfrac{1}{2}\frac{\partial w_e}{\partial t}+\tfrac{1}{2}q\frac{\partial Q}{\partial y}=0 \qquad (2.3.7)$$

and

$$\frac{\partial(q^{1/2}T_e^{-1}\bar{d})}{\partial t}-\tfrac{1}{2}\frac{\partial w_e}{\partial t}+\frac{\partial\bar{B}}{\partial y}=0, \qquad (2.3.8)$$

where

$$\bar{B}=\tfrac{1}{2}q[T_e^{-2}\bar{d}^2+T_e^2(\bar{d}-q^{-1})^2]+\bar{d}+h \qquad (2.3.9)$$

and

$$Q=2\bar{d}^2. \qquad (2.3.10)$$

Note that the two dependent variables are now $\bar{d}$ (equivalent to half the depth at the right wall) and the stream width w_e (as contained in T_e). Equations (2.3.7) and (2.3.8) can be interpreted as momentum and continuity relations for the cross-sectional flow as a whole.

It is possible to write (2.3.7) and (2.3.8) in characteristic form (Stern et al, 1982) and to show that the characteristic speeds are given by (2.2.22) with $\hat{d}=\bar{d}$ and w=w_e (Kubokawa and Hanawa, 1984a). The Riemann invariants cannot be obtained in closed form and must be determined numerically (Stern et al. 1982). In the interest of simplicity, we will explore two limiting cases, those of narrow and wide stream widths compared with L_d. The narrow-channel limit again corresponds to $q\rightarrow 0$, now with w_e fixed, and was first described by Stern (1980). The depth and velocity profiles can be obtained as limiting cases of (2.3.1) and (2.3.2), or simply by solving (2.1.14) with q=0. The resulting depth and velocity profiles are given by

$$d = \frac{(x - \frac{1}{2}w + w_e)}{\frac{1}{2}w_e}\bar{d} - \frac{1}{2}(x - \frac{1}{2}w)(x - \frac{1}{2}w + w_e), \tag{2.3.11}$$

and

$$v = \bar{v}(y,t) - x + \frac{1}{2}w - \frac{1}{2}w_e, \tag{2.3.12}$$

with

$$\bar{v} = 2\bar{d}/w_e \tag{2.3.13}$$

A more natural representation of the depth can be found in terms of the distance $x' = x - \frac{1}{2}w + w_e$ measured from the free edge of the current (see Figure 2.3.1a). This replacement leads to

$$d = x'(v_e - \frac{1}{2}x'), \tag{2.3.14}$$

where

$$v_e = \bar{v} + \frac{1}{2}w_e. \tag{2.3.15}$$

The velocity is given by $v(x,y) = v_e(y) - x'$. When extended past the wall, as shown in Figure 2.3.1a, the depth profile is a parabola with a maximum value $d_{\max} = \frac{1}{2}v_e^2$. The shape of the profile is independent of the position of the wall and variations of the profile with *y* or *t* can be thought of as a combination of lateral displacement with respect to the wall (due to changes in w_e) and uniform expansion or contraction of the profile (due to changes in v_e). When $w_e > v_e$ (Figure 2.3.1b) the depth has a maximum to the left of the wall implying negative *v* along the wall and positive *v* further offshore. When $w_e < v_e$, as in Figure 2.3.1c, there is no depth maximum and v>0 across the entire stream.

The equations governing the evolution of the above profiles in *y* and *t* can be obtained from (2.3.7) and (2.3.8) in the limit of small *q*. Use of the expansion

$$T_e \approx q^{1/2}\frac{w_e}{2} - \frac{1}{3}\left(q^{1/2}\frac{w_e}{2}\right)^3 + \cdots$$

in (2.3.7) along with the relation $\bar{d} = \frac{1}{2}w_e(v_e - \frac{1}{2}w_e)$ leads to

$$\frac{\partial}{\partial t}\left[w_e^2(v_e - \frac{1}{3}w_e)\right] + \frac{\partial}{\partial y}2Q = 0 \tag{2.3.16}$$

where $Q = \frac{1}{2}\left[w_e(v_e - \frac{1}{2}w_e)\right]^2$. In addition, the value of *B* is uniform for *q*=0 and this allows (2.3.6) to be written as

$$\frac{\partial}{\partial t}(v_e - w_e) + \frac{\partial}{\partial y}\overline{B} = 0 \qquad (2.3.17)$$

where $\overline{B} = \frac{v_e^{\ 2}}{2} + h$.

Equations (2.3.16) and (2.3.17) may be written in the standard characteristic form[1] with

$$c_\pm = \frac{v_e - w_e}{1 \mp [w_e/(2v_e - w_e)]^{1/2}} \qquad (2.3.18)$$

and

$$R_\pm = \int^{v_e/w_e} \frac{1}{1 - \xi - \dfrac{2\xi}{1 \pm (2\xi - 1)^{1/2}}} d\xi - \ln(w_e). \qquad (2.3.19)$$

$R_\pm$ is conserved following the characteristic speed $c_\pm$, provided that h=constant. Note that both characteristic speeds are zero for $w_e=2v_e$, corresponding to the case in which the right wall depth is zero (the flow is separated from both walls). The right wall depth is finite for $0< w_e<2v_e$ and careful evaluation of (2.3.18) shows that c_+ is always >0 over this range. The behavior of c_- is more complicated, with $c_-<0$ for $v_e<w_e<2v_e$ and $c_->0$ for $w_e<v_e$. Thus, the flow is subcritical ($c_+>0$ and $c_-<0$) when $v_e<w_e<2v_e$, in which case the depth profile resembles that of Figure 2.3.1b (with reverse velocity along the right wall). The flow is supercritical ($c_\pm>0$) when $w_e<v_e$, in which case the depth profile resembles that of Figure 2.3.1c and the velocity is unidirectional. The different possibilities are shown as insets in Figure 2.3.2.

Insight into various wave forms and transient motions can be gained by looking at a plot of the Riemann functions in (w_e,v_e) space (Figure 2.3.2). The solid contours correspond to constant R_+ or R_-, as labeled. The curves terminate at the diagonal $v_e=w_e/2$, along which $c_\pm = 0$ and below which the flow is separated from both walls. Paldor (1983) has shown that this doubly separated state is unstable[2]. Slightly above is a second diagonal $v_e=w_e$ along which the flow is critical, $c_-=0$ (and $c_+>0$). In the wedge shaped region between these two lines the flow is subcritical and above it the flow is supercritical. Contours of constant c_+ correspond to dashed contours. Figure 2.3.3 shows part of the same parameter space with contours of constant c_-.

---

[1] The characteristic speeds can also be written as $c_\pm = \overline{v} \pm \overline{d}^{1/2}$, which was the expression obtained for the characteristic speeds in a nonseparated flow. The ± sign has been reversed from how it appears in Stern (1980) so that the '-' waves are the only ones with the ability to propagate upstream.

[2] Paldor has shown that the flow is provably stable for $v_e>3w_e/2$. Also, by his direct numerical calculation of eigenfunctions, he has shown that the flow is stable for $3w_e/2>v_e>w_e/2$. At $v_e=w_e/2$ the entire flow separates and, as we have shown, both long waves take on the same speed (zero). Resonance between these two waves produces an instability. This subject is taken up in a more general context in Section 3.9.

The orientation of the curves of constant R_+ and R_- gives clues concerning the differences between the '+' and '-' waves. Over most of the (w_e,v_e)-plane, the R_+=constant curves tend to be horizontal whereas the R_-=constant curves tend to be more vertical. Variations in R_- therefore tend to be associated more with variations in the stream width; that is, lateral shifts of the fixed depth profile relative to the right wall, as explained in connection with Figure 2.3.1. We therefore refer to the corresponding disturbances as *frontal waves*. Variations in R_+ tend to be associated more with variations in v_e that, in turn, are associated with uniform expansions of the depth profile. Plots of Riemann invariants for finite values of q (e.g. Stern et al. 1982) display the same tendencies. Frontal waves are sometime referred to as Kelvin waves in the literature, but their signature lateral motion is more characteristic of potential vorticity waves.

Now consider a transient disturbance that has R_-=constant and therefore consists only of forward propagating signals-those assigned the '+' sign. An initial state for this 'simple wave' can be constructed by choosing $v_e(y,0)$ and calculating $w_e(y,0)$ by tracing along a particular R_-=constant curve in Figure 2.3.2. Suppose that we use the initial distribution shown in Figure 2.3.4a, where v_e decreases with increasing y. Also suppose that this distribution spans the segment **AB** of Figure 2.3.2. Since both $R_-(w_e,v_e)$ and $R_+(w_e,v_e)$ are constant following the characteristic speed c_+ for this initial condition, w_e and v_e must be individually be conserved. The value of w_e is nearly constant along **AB** and therefore the variation in cross section from **A** to **B** is primarily one in wall depth (Figure 2.3.4a). From the contours of c_+ shown in Figure 2.3.2, all of which have positive values, the characteristic speed corresponding to **A** is larger than that associated with **B.** Therefore the *entire profile* at **A** will move more rapidly in the positive y-direction than the **B** profile, resulting in wave steepening (Figure 2.3.4b).

Next consider a case in which the '+' waves are filtered out of the flow by a choice of initial condition with R_+=constant. The remaining frontal waves are associated more with variations in w_e than in v_e and it therefore makes sense to choose $w_e(y,0)$ and calculate the corresponding $v_e(y,0)$. The latter can be accomplished by tracing along the R_+=constant curve shown in Figure 2.3.3. Consider the initial condition shown in Figure 2.3.5a, with $dw_e(y,0)/dy<0$. As shown by the dashed contours of Figure 2.3.3, the behavior of c_- is somewhat more complicated than that for c_+. If the initial condition spans the segment **CD**, then c_- is negative with larger absolute values associated with smaller widths. In this case the frontal wave will propagate to the left and steepen, as in Figure 2.3.5b. On the other hand, an initial condition of the same general shape and spanning the segment **EF** will rarefy, as suggested in Figure 2.3.5b.

An example of steepening of the 'frontal ' wave is shown in Figure 3.4.12. The wave is generated in the region $4<y<7$ of the t=10 frame, where the current widens. The current is supercritical and the narrow and wide end states correspond to something like points **G** and **H** in Figure 2.3.3. The narrower, upstream end state propagates forward and the greater speed in this case and overtakes the wider portion (t=20 frame near y=10) eventually leading the near detachment of a blob of fluid (t=40).

The other limiting case is that of a relatively wide stream, w_e*>>L_d (or $q^{1/2}w$>>1). Here the Kelvin wave trapped to the right wall of the channel is isolated from the free edge of the stream and therefore the propagation speed is given by the formula (2.2.25) for attached flow. The frontal wave is trapped to the free edge and has properties quite different from those of the left wall Kelvin wave that it replaces. These new features are revealed by examining (2.3.6), the momentum equation for the flow at the free edge. The velocity v_e can be found by taking the limit of (2.3.2) as $q^{1/2}w\rightarrow\infty$ and evaluating the result at the free edge, leading to $v_e=q^{-1/2}$. The free edge velocity is constant and thus (2.3.6) gives

$$\frac{\partial w_e}{\partial t}=0 \qquad (h\text{=constant}).$$

Any initial distribution $w_e(y,0)$ therefore remains frozen in the flow, implying that the characteristic speed for such disturbances, c_-, is zero. A wide, separated flow over a horizontal bottom is therefore always critical with respect to a frontal wave.[3]

Figure Captions

Figure 2.3.1 Possible cross sections for separated flow with zero potential vorticity.

Figure 2.3.2 Riemann invariants and characteristic speeds for separated, zero potential vorticity flow. Solid contours show constant values of R_+ and R_-, as indicated by a '+' or '-'. The dashed curves show values of the characteristic wave speed c_+. The insets show different states of criticality corresponding to particular cross sections. (Based on a similar figure in Stern 1980).

Figure 2.3.3 Same as Figure 2.3.2 but showing contours of the characteristic speed c_-.

Figure 2.3.4 The evolution of a modified gravity wave (with uniform R_-) for which the initial distribution of the free-edge velocity is specified.

Figure 2.3.5 The evolution of a frontal disturbance (with uniform R_+) for which the initial distribution of the free-edge position is specified.

[3] Cushman-Roisin, Pratt and Ralph (1993) have explored the slow evolution of the frontal waves in a wide flow when weak dispersive effects are introduced. Expansion in powers of the aspect ratio δ shows that the free edge of the stream is governed by the modified Korteweg-de-Vries equation. As it turns out, only propagation in the positive y-direction is permitted.

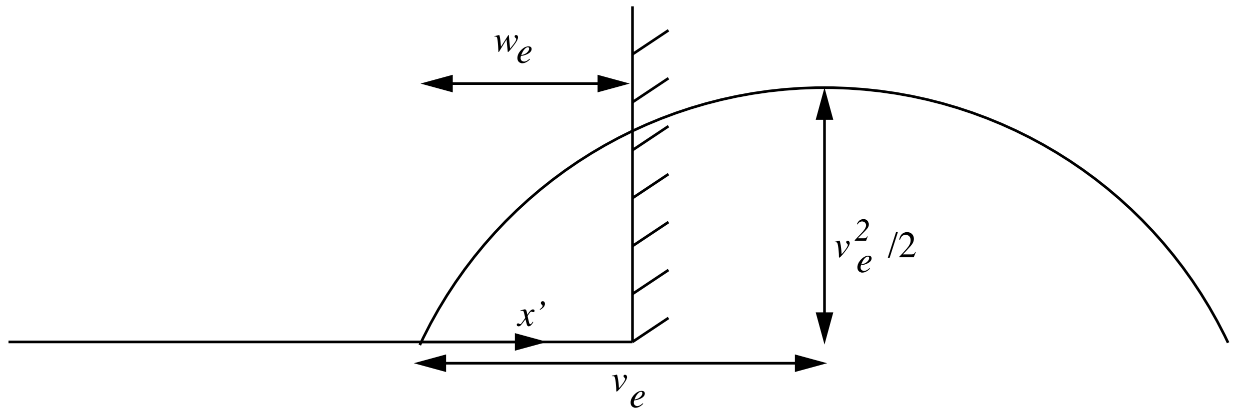

(a)

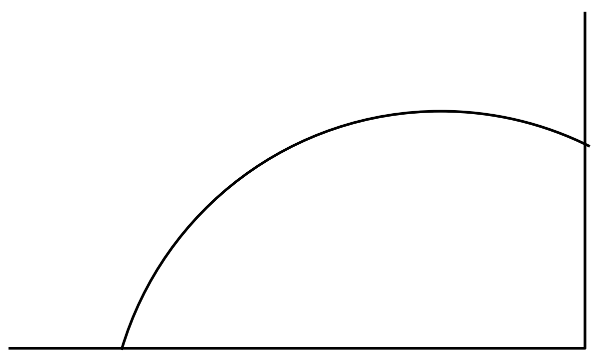

(b)

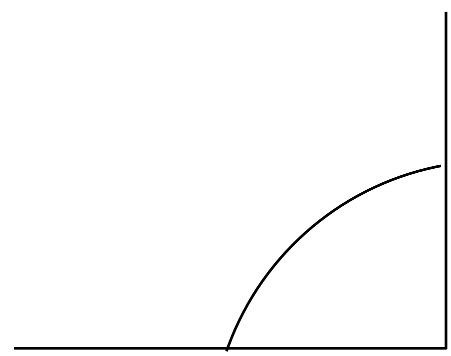

(c)

Figure 2.3.1

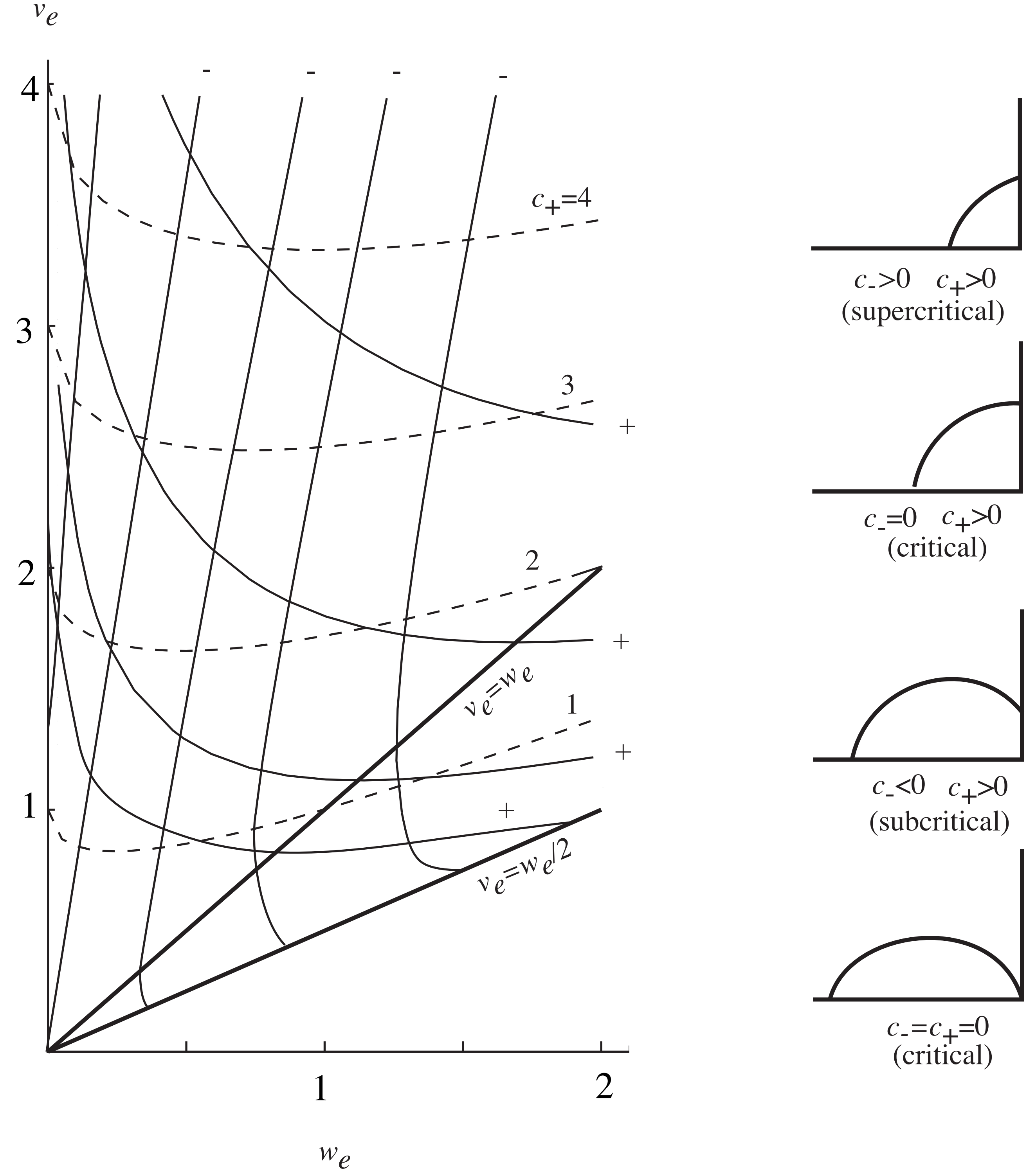

v_e
4
3
2
1
1
2
w_e
$c_+=4$
3
2
1
+
+
+
+
-
-
-
-
$v_e=w_e$
$v_e=w_e/2$
$c_->0$ $c_+>0$
(supercritical)
$c_-=0$ $c_+>0$
(critical)
$c_-<0$ $c_+>0$
(subcritical)
$c_-=c_+=0$
(critical)

Figure 2.3.2

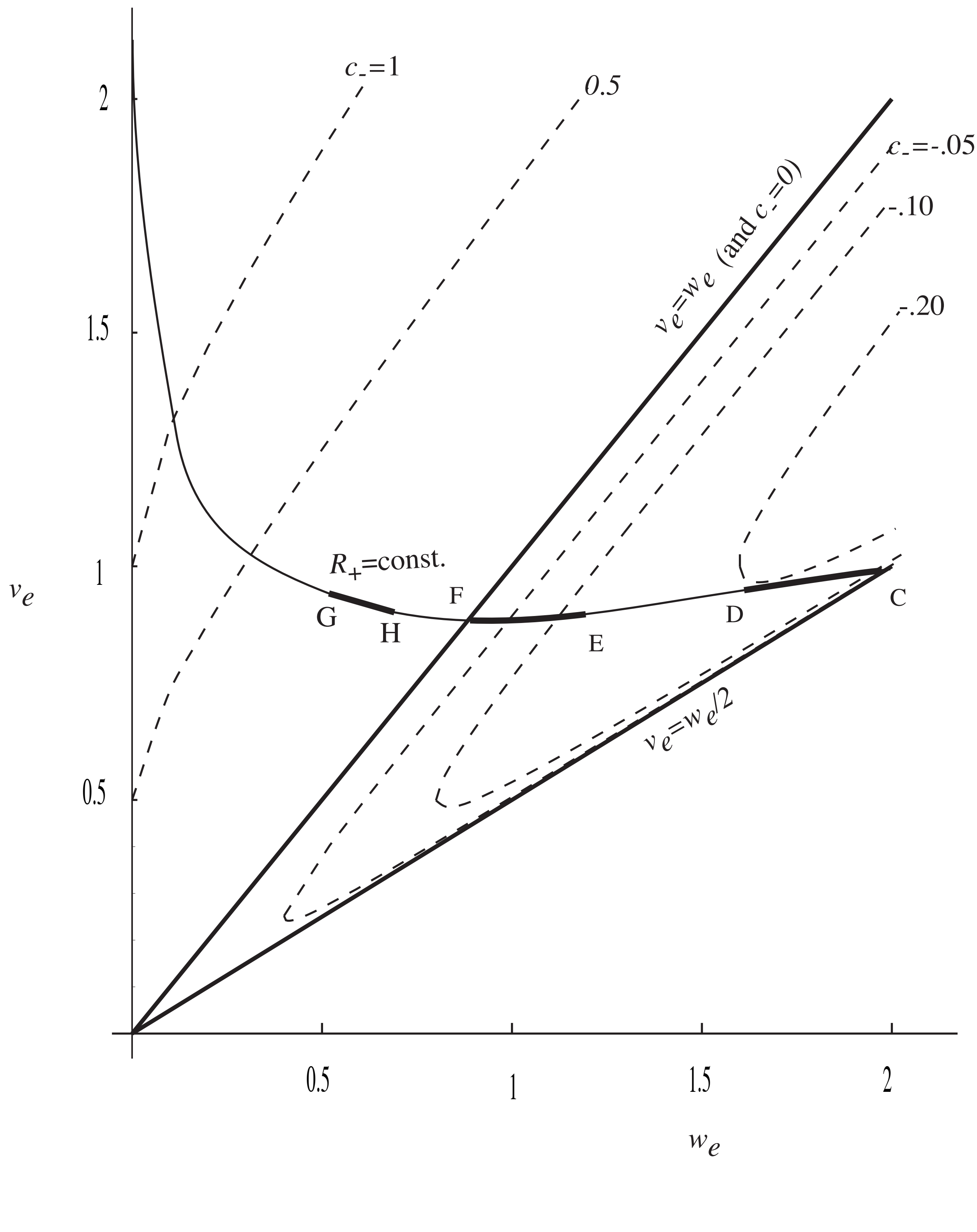
c_-=1
0.5
c_-=-.05
-.10
-.20
v_e=w_e (and c_-=0)
R_+=const.
v_e=w_e/2
G
H
F
E
D
C
2
1.5
1
0.5
v_e
0.5
1
1.5
2
w_e

Figure 2.3.3

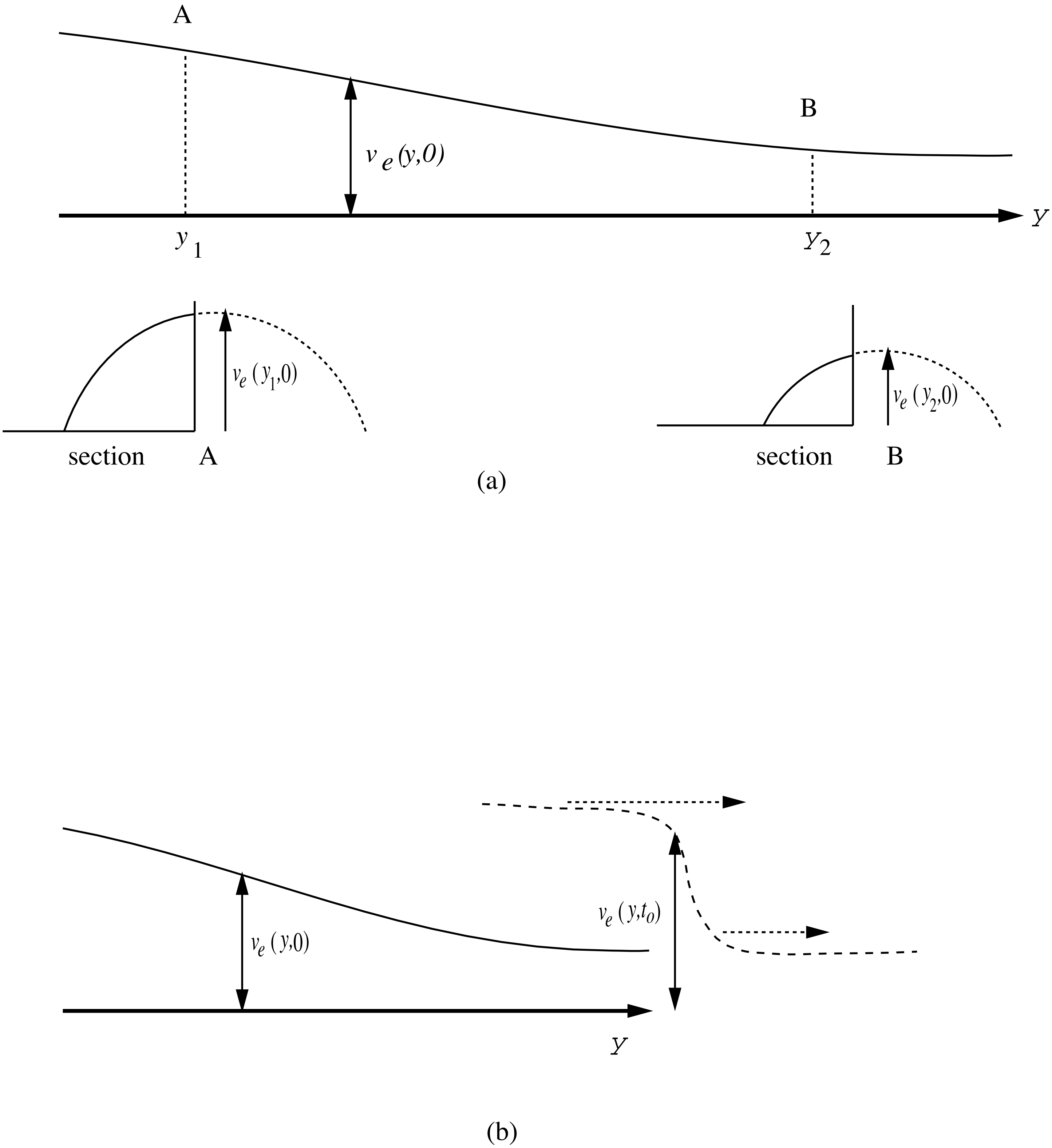

Fig. 2.3.4

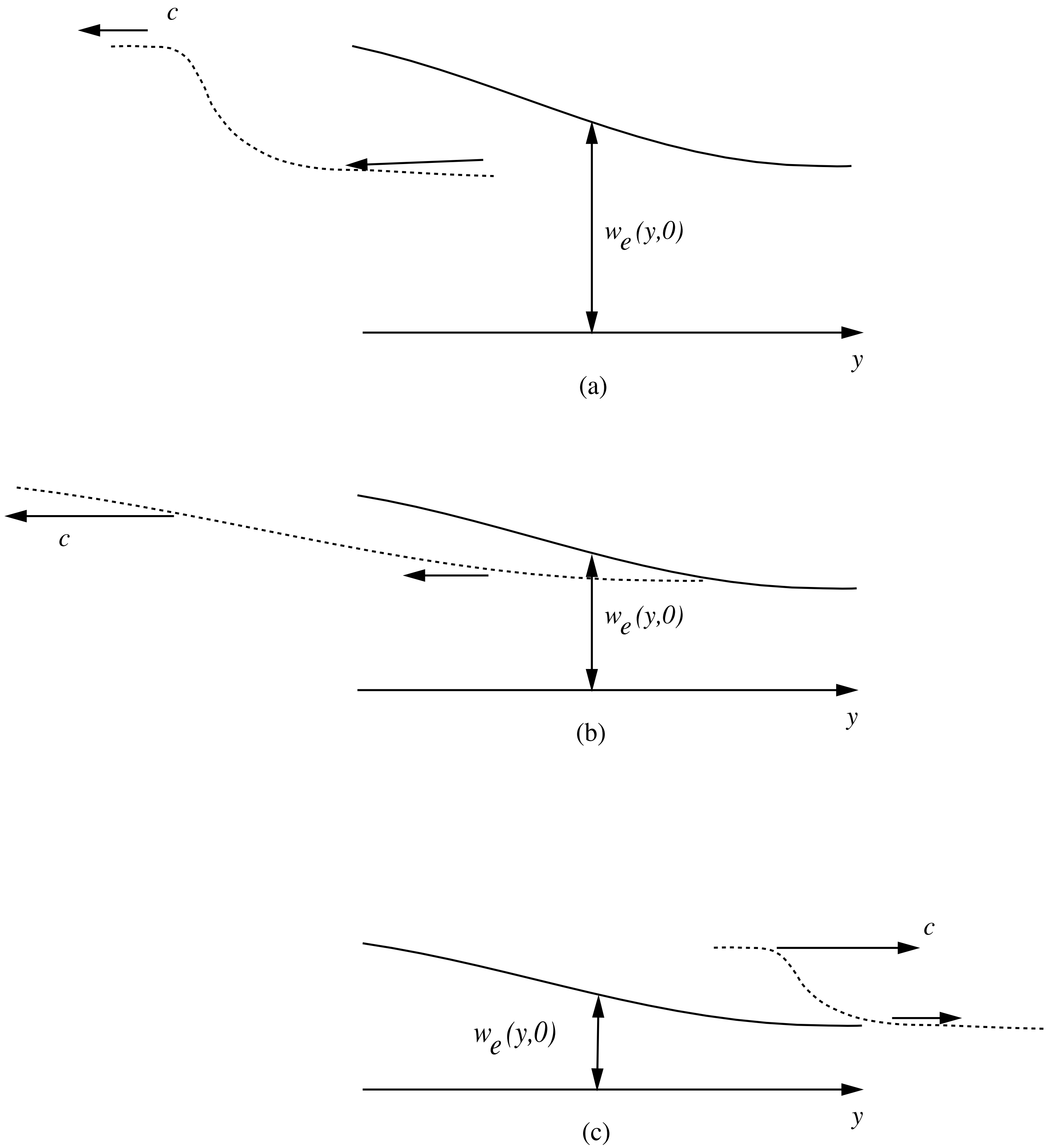

Figure 2.3.5